Study of growth parameters for single InAs QD formation on GaAs (001) patterned substrates by local oxidation lithography.

Jesús Herranz, Luisa González, Lukasz Wewior, Benito Alén, David Fuster, and Yolanda González

IMM-Instituto de Microelectrónica de Madrid (CNM-CSIC), Isaac Newton 8, PTM, E-28760 Tres Cantos, Madrid, Spain

ABSTRACT. This work studies the selective nucleation of InAs within nanoholes on GaAs (001) substrates patterned by atomic force microscopy local oxidation. The effects of substrate temperature and As_4 overpressure during InAs deposition directly on the patterned substrate (without GaAs buffer layer) are considered. It is found that when InAs is deposited at substrate temperature of 510ºC under low As_4 overpressure, a single InAs quantum dot per nanohole is obtained for a broad range of sizes of pattern motifs. The use of these InAs quantum dots as seed nuclei for vertical stacking of optically active single InAs site-controlled quantum dots is investigated.

1. Introduction

The capability to systematically address individual nanostructures is an important technological goal towards the scalable fabrication of novel devices that exploit single nanostructure properties[1]. Using semiconductor quantum dots (QDs) as sources of quantum light states, such as single photon sources or entangled photon pair sources, integrated in photonic circuits is a promising pathway for the implementation of quantum communication and quantum computation schemes at the microscale[2]. Among other semiconductor systems, InAs/GaAs system has been widely studied because of the high quality QDs obtained by epitaxial Stranski-Krastanov self-assembled processes. One limiting feature of the self-assembled process is the lack of control of the location of the nanostructures. In this the sense, the growth of InAs QDs on patterned substrates has emerged as a powerful strategy[3], being currently a research topic of increasing interest. Nanoholes patterned on a flat substrate surface define preferential InAs nucleation positions, which are associated with local minimums of the surface chemical potential at the bottom of each nanohole. Different lithographic techniques have been demonstrated as suitable for the fabrication of nanohole patterned substrates, including e-beam lithography[4-6], nanoimprint lithography[7] or laser interference lithography[8]. Other techniques such as focus ion beam (FIB) patterning[9] and atomic force microscopy (AFM) oxidation lithography[10-12] have also been developed.

It is remarkable the great improvements on the optical quality of positioned InAs nanostructures achieved in recent years[13-16] demonstrating site-controlled InAs QDs that match the optical properties of self-assembled InAs QDs with a yield of ~20%[15]. Nevertheless, a deeper knowledge of the nucleation process of InAs on patterned substrates is still needed. A better understanding of the growth kinetics could enable the development of high optical quality site-controlled quantum dots (SCQDs) fabrication processes with improved throughput.

In this work, we use GaAs (001) patterned substrates fabricated by AFM local oxidation lithography as templates for growth of site-controlled InAs QDs. This lithography technique has been demonstrated as a powerful tool for substrate patterning[10-12]. It provides high positioning accuracy and it is very promising in novel strategies for deterministic integration of single nanostructures in photonic cavities[17,18] for future quantum information applications. Here, we report on the influence of two main parameters during growth by molecular beam epitaxy (MBE), namely substrate temperature and As_4 overpressure, on the InAs nucleation process within patterned nanoholes. The study focuses on the number of InAs QDs obtained per pattern site and nucleation kinetics. It is found that high substrate temperature prevents the formation of InAs 3D nuclei within nanoholes due to changes in In incorporation and that, interestingly, nanohole occupancy is affected by the As_4 overpressure conditions. Single InAs QD nucleation within the nanoholes is achieved under low As_4 flux conditions at substrate temperature (T_S) of 510 ºC in a wide range of pattern site dimensions, in contrast with multiple InAs QD nucleation observed when higher As_4 flux is employed.

2. Experimental details

The samples were grown on epitaxial GaAs (001) substrates, consisting of 500 nm thick GaAs layers grown on epi-ready commercial substrates by MBE at a growth rate (r_g) of Ga of 1ML/s, T_s=580 ºC and V/III flux ratio equal to 8. Epitaxial substrates are kept in nitrogen atmosphere until the pattern fabrication in order to preserve the GaAs surface.

Patterning of the GaAs(001) substrates was performed by AFM local oxidation lithography, operating a Nanotec commercial AFM system in dynamic mode in ambient conditions (RH-20-30%). n-doped Nanosensors Si AFM tips with a resistivity of 0.01-0.02 Ωcm and tip radius of

~7nm were used. The resonance frequency and force constant of the cantilevers were f=270 kHz and K=40Nm^{-1}, respectively. Fabricated patterns consist of square arrays of GaAs oxide point motifs with a 2μm pitch. A 2μm pitch produces a low QD density, suitable for single QD integration in optical photonic cavities. Dimensions of oxide pattern motifs were changed by varying both voltage and oxidation time. The oxide patterns considered in this work were fabricated with oxidation voltage (V_{ox}) and oxidation time (t_{ox}) in the range V_{ox}=15-20V and t_{ox}=50-5000ms, respectively. With this AFM set-up positioning accuracy ~50nm is achieved [17]. This value is limited by drift in the movement during the lithography step; however it is important to remark that this is not an intrinsic limitation of the technique itself and can be improved in current commercially available AFM setups with advanced non-linearity piezo correction. Scratched alignment marks are used for localization of the patterned regions with the integrated optical set-up of the AFM system. Therefore, patterned regions can be scanned after epitaxial growth to individually relate the oxide motif geometry with the obtained InAs nanostructures.

Nanoholes patterns are obtained by selective removal of the fabricated oxides patterns in a HF wet etching step (HF 50%, 5minutes). Immediately after HF wet etching, samples are In bound to the substrate holder and introduced inside the MBE system. Subsequent epitaxial growth starts with the native oxide desorption under atomic H. The surface sample is exposed during 30 minutes to an atomic H flux, obtained by thermal cracking of H_2, at a base pressure of H_2 P=4.5·10^{-5} Torr at T_S=450ºC in the MBE growth chamber. Simultaneously to the atomic H flux, As_4 is supplied at beam equivalent pressure, BEP (As_4)=6.4·10^{-6} Torr. GaAs oxides species are reduced to species volatile at lower T_S than conventional thermal oxide desorption temperatures[19,20]. This process efficiently removes the surface oxide and provides a clean surface

suitable for epitaxial re-growth[21]. Atomic H treatment is monitored by reflection high energy electron diffraction (RHEED). Specular spot shows up in less than 2 minutes after the H treatment starts and a 2x RHEED pattern along [1-10] direction is observed during this cleaning treatment. Once the cleaning process is completed, sample temperature is increased to that of InAs deposition in 8 minutes with As_4 cell closed. A (2x4) GaAs surface reconstruction RHEED pattern is observed during this step. InAs is then directly (without previous GaAs buffer layer growth) deposited on the patterned substrate surface at r_g(In)~0.01ML/s. A two minutes long annealing step under As_4 flux is performed in all samples after InAs deposition.

In this work, substrate temperature is calibrated using the well-known surface GaAs reconstruction transition between a (2x4) and c(4x4)[22]. Under fixed As_4, this reconstruction transition takes place at a known substrate temperature. In particular, we used an As_4 flux equivalent to 2ML/s of As, for which the transition is observed at T_S=520ºC. The As_4 flux is calibrated on flat substrates by RHEED oscillations under Ga-rich growth conditions at low enough T_S (~460ºC) for avoiding simultaneous As desorption[23]. From this point on, we will refer to As_4 fluxes in terms of their equivalence to monolayers per second (ML/s) of As on a GaAs (001) surface (F_{eq} (As)).

The influence of T_S and As_4 overpressure on InAs nucleation on patterned motifs was studied in two series of samples. In one series, a F_{eq}(As) =2ML/s was set and three different substrate temperatures (T_S=490ºC, T_S=510ºC and T_S =530ºC) were explored. In the other series, substrate temperature was set to T_S=510ºC and three different As_4 fluxes (F_{eq}(As) =0.5ML/s, F_{eq}(As)=2ML/s and F_{eq}(As)=3.5ML/s) were employed.

Morphological characterization of samples was performed by AFM using the same Nanotec set-up employed for substrate patterning. Nanosensors Si AFM tips with nominal tip radius of 7 nm were employed. Photoluminescence (PL) characterization of the obtained nanostructures was

performed at 4K using a diffraction limited confocal microscope inserted in a low vibration cryogen free cryostat (Attocube Attodry 1000). A 785nm continuous wave diode laser was used to excite the photoluminescence which was dispersed by a 750 mm focal length spectrometer at a resolution of ~30 μeV and detected with a cooled Si Charge Coupled Device (CCD). A XY piezo scanner was used to record scanning PL maps.

3. Results and discussion

Figure 1 presents 2x2 motifs pattern AFM images corresponding to the main steps of the site-controlled InAs QDs fabrication process. A schematic drawing of each step is shown at the top. Figure 1a shows the oxide motifs fabricated by AFM local oxidation lithography. GaAs oxides generated in the AFM local oxidation process expand above and below the semiconductor surface. Figure 1b shows corresponding nanoholes obtained by HF selective removal of the fabricated oxides. Figure 1c shows four nanoholes after the atomic H treatment and thermal ramp step in the MBE growth chamber, which correspond to the situation of the nanoholes right before InAs deposition. Nanohole shape is no longer circular, due to the morphological evolution during the thermal ramp that leads to elliptical nanoholes elongated along [110] crystallographic direction (inset in figure 1c clearly shows the elongated nanohole shape, in contrast to the circular nanohole obtained after HF wet etching shown in the inset in figure 1b). Figure 1d presents InAs nanostructures selectively nucleated at the four pattern sites.

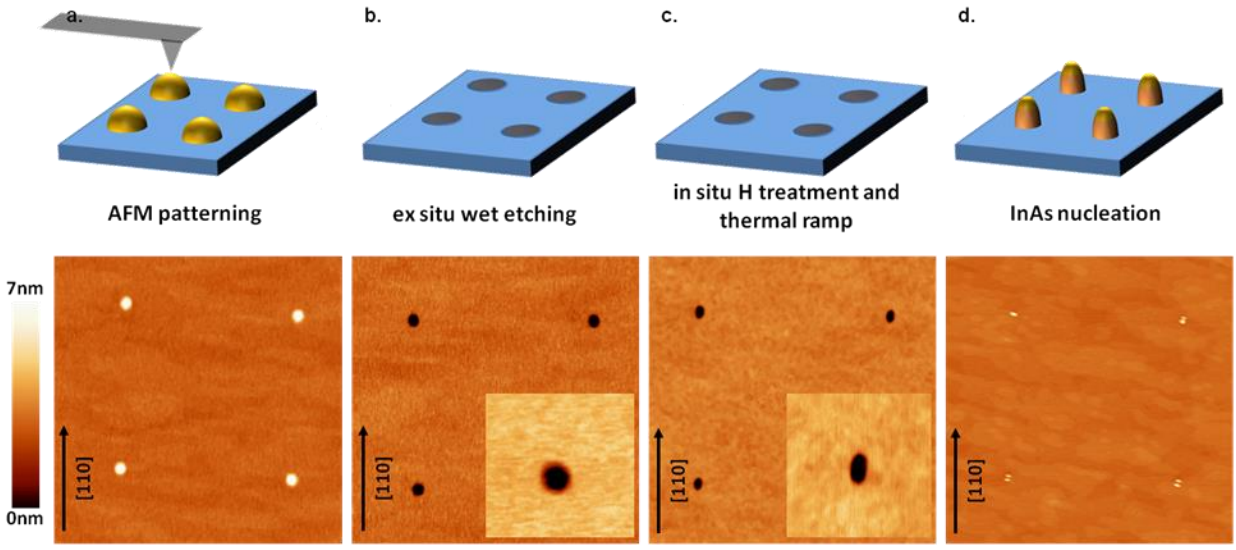

Figure1. Schematics of the fabrication process steps for site-controlled InAs nanostructures with corresponding 3x3 μm ^{2} atomic force microscopy (AFM) images showing 2x2 motifs: local oxidation AFM patterning of epitaxial GaAs (001) substrate (a), nanoholes obtained after 5 minutes HF wet etching (b) nanoholes after in-situ atomic H treatment at T_S=450ºC and subsequent thermal ramp to T_S=510ºC (c) and InAs nucleation. Same color scale was used in the four AFM images. 800x800nm^2 AFM inset images with enhanced color scale are included to clearly show the shape evolution of the nanoholes previous to InAs deposition.

3.1 Effect of temperature on the nucleation of InAs on patterned surface substrate

We first look at the effect of growth temperature on the InAs nucleation. Substrate temperatures T_S=490ºC, T_S=510ºC and T_S=530ºC, with a fixed F_{eq}(As)=2ML/s, were studied. Under this As_4 pressure, GaAs surface shows a c(4x4) reconstruction for T_S=490ºC and T_S=510ºC , while a (2x4) structure is observed for T_S=530ºC. It is well known that an increase of the substrate temperature implies an increase of the apparent InAs critical thickness for QD formation on flat surfaces, i.e. an increase of the nominal quantity of InAs deposited to observe the onset of tridimensional islands formation. A decrease of In sticking coefficient with

temperature above T_S=500ºC has been pointed out as a key factor to explain this effect[24,25]. Indium desorption also becomes a relevant mechanism in the considered temperature range[26]. In order to grow the same InAs material quantity, the deposition time was adjusted for each substrate temperature and set to 88% of that corresponding to the critical thickness for InAs QD formation on flat GaAs (001) surfaces, as observed by RHEED. This means an increment on the In deposition time of 13% for T_S=510ºC and 51% for T_S=530ºC with respect to that employed at T_S=490ºC at the chosen In deposition rate (r_g(In)~0.01ML/s).

Figure 2 presents the results obtained for InAs grown at the three substrate temperatures (2a for T_S=490ºC, 2b for T_S=510ºC and 2c for T_S=530ºC) on pattern sites of similar oxide motif geometry. AFM images and the corresponding profiles along [110] (red line) and [1-10] (blue line) crystallographic directions are shown. Oxide motif profile and its negative are included as a reference (black lines). Multiple nucleation within pattern sites is observed on the samples grown at T_S=490ºC (figure 2a) and T_S=510ºC (figure 2b), with InAs QDs aligned along [110] direction. We have previously reported this alignment[27] and it has also been observed by other groups[16,28]. It is due to the preferential incorporation of In on B-type faces (As-terminated) within elongated motifs under these growth conditions. In this work, motif asymmetry results from the shape evolution of the nanoholes during the regrowth steps previous to InAs deposition: oxide desorption at T_S=450ºC during 30 minutes and thermal ramp from T_S=450 ºC up to T_S employed for InAs deposition in each sample. Although nanoholes obtained after HF etch are symmetrical (replicating oxide dimensions), preferential Ga atoms migration towards B-type (As terminated) facets from the flat surface and away from A-type facets (Ga terminated) produce elliptical motifs elongated along [110] direction. It is important to point out that no GaAs buffer layer was grown, the evolution of nanohole shape occurs due to thermal activated Ga transport across the surface[29]. The sample grown at T_S=530ºC (figure 2c) shows a different behavior. Pattern motifs have been partially filled after InAs growth, although no tridimensional nuclei are found over surface level. Pattern sites are revealed in the AFM scans by ~1nm depressions arranged with the 2 μm periodicity of the fabricated pattern substrates (shown in the inset in figure 2c with enhanced color scale). The observed behavior could be due to strong In reevaporation from the surface during the 2 minutes annealing step after InAs deposition, dissolving the three-

dimensional islands grown on pattern sites. Fast dissolution of InAs self-assembled QDs has been reported when T_S is increased up to 535ºC[30]. It is important to point out that the reproducibility of the growth at T=530ºC is limited by the critical dependence of In incorporation at this temperature on As pressure; small variations in T_S (smaller than the T_S reproducibility in MBE systems) and/or in As_4 overpressure during a growth run could give rise to important changes in the actual quantity of incorporated In.

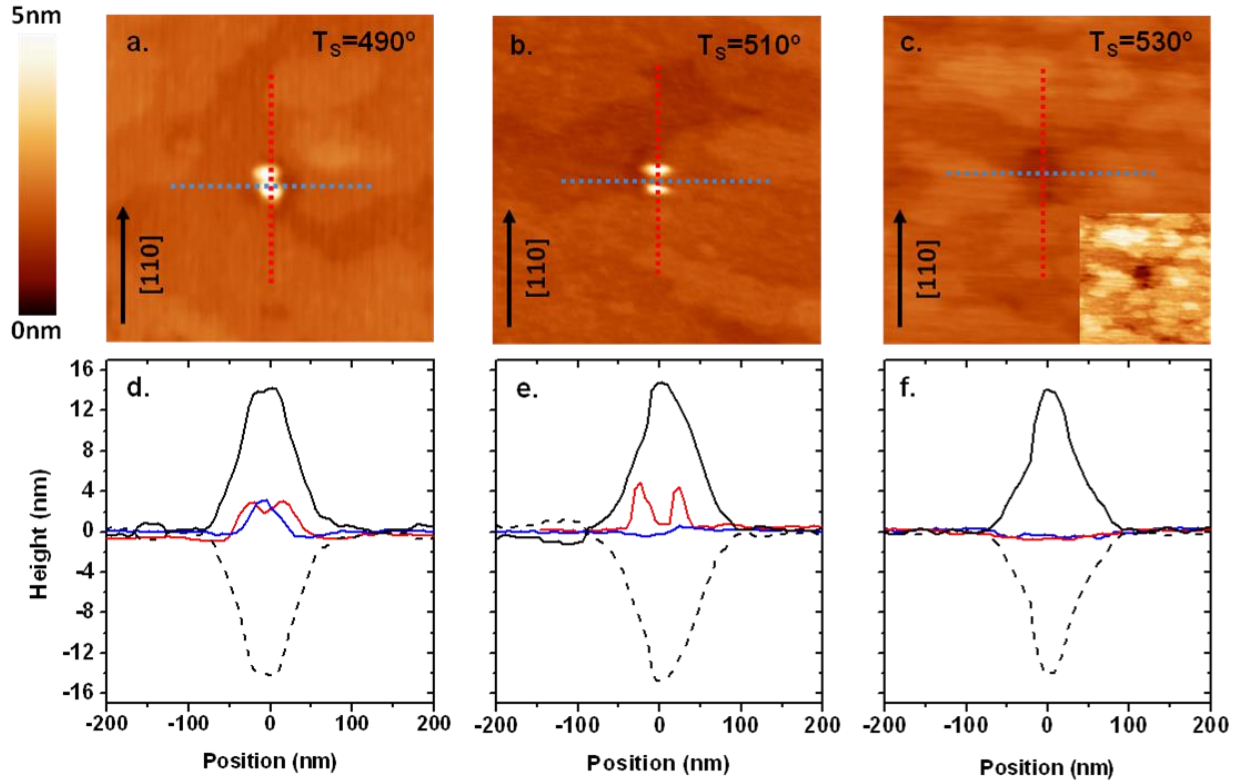

Figure 2. Atomic force microscopy (AFM) images (800x800nm^2) of positioned nanostructures grown at substrate temperature equal to T_S=490ºC (a), T_S=510ºC (b) and T_S=530ºC (c) on AFM local oxidation patterned substrates. Same color scale is used in the three images (inset: smaller area scan with enhanced color scale). Corresponding AFM profiles (d-f) along [110] (red) and [1-10] (blue) crystallographic directions (indicated in the AFM images with dashed lines) are shown at the bottom. Original oxide profile (black solid) and negative oxide profile (black

dashed) are also included as a reference. Pattern oxide motifs with similar geometry were chosen for results comparison.

3.2 Effect of As_4 overpressure on the nucleation of InAs on patterned surface substrate

Next, we consider the effect of As_4 overpressure on InAs selective nucleation process for T_S=510ºC. As_4 fluxes of F_{eq}(As)=0.5ML/s, F_{eq}(As)=2ML/s and F_{eq}(As)=3.5ML/s were studied. At this substrate temperature, the GaAs surface shows a (2x4) reconstruction for F_{eq}(As) =0.5ML/s and a c(4x4) for F_{eq}(As)=2ML/s and F_{eq}(As)=3.5ML/s. In this sample series, an identical InAs coverage was deposited, being equal to 88% of the critical thickness for InAs QD formation on flat GaAs(001) surfaces at T_S=510ºC under F_{eq}(As)=2ML/s, as observed by RHEED. Nanostructures grown under the different As_4 fluxes studied obtained in pattern sites of similar oxide geometry are presented in figure 3. AFM images and the corresponding profiles along [110] (red lines) and [1-10] (blue lines) direction are shown. Oxide motif profile and its negative are included as a reference (black lines). For the lowerAs_4 flux, single QD formation is achieved with QD placed at the bottom of the pattern nanohole, while multiple QD formation is observed at higher As_4 flux, with QDs aligned along [110] direction.

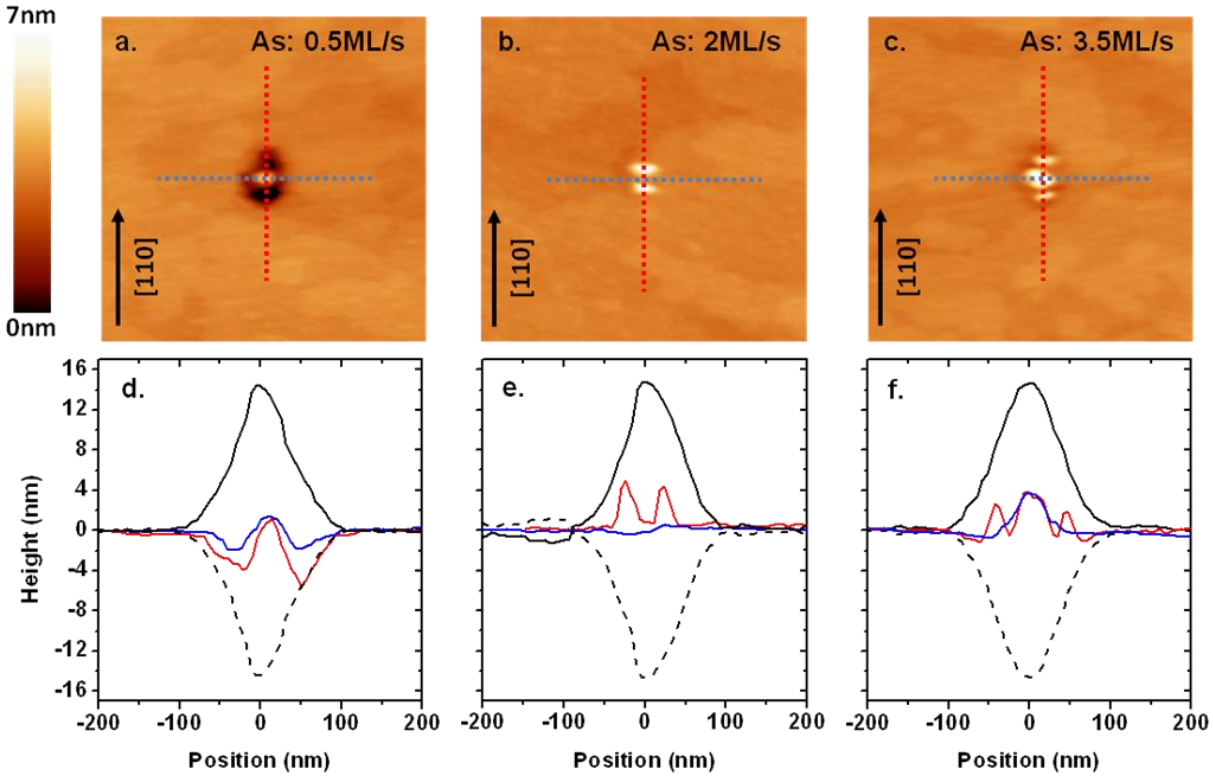

Figure 3. Atomic force microscopy (AFM) images (800x800nm^2) of positioned nanostructures grown with As_4 flux equal to F_{eq}(As)=0.5ML/s (a), F_{eq}(As)=2ML/s (b) and F_{eq}(As)=3.5ML/s (c) on AFM local oxidation patterned substrates. Same color scale is used for the three images. Corresponding AFM (d-f) profiles along [110] (red) and [1-10] (blue) crystallographic directions (indicated in the AFM images with dashed lines) are shown. Original oxide profile (black solid) and negative oxide profile (black dashed) are also included as a reference. Pattern oxide motifs with similar geometry are chosen for results comparison.

For understanding these results, different aspects involved in the InAs nucleation have to be taken into account. First, the motif geometry is a key factor in the growth on patterned substrates, as one term of the surface chemical potential for incoming species is proportional to surface

curvature[31]. The concave shape at the bottom of a nanohole constitutes a local minimum of the surface chemical potential that drives a net In flux towards the hole. This leads to reach the critical volume for nucleation of InAs QD within the pattern sites earlier than on a flat surface. Second, the high step density at the sidewalls of the hole is also key to explain the preferential nucleation of InAs at the pattern sites, as In adatoms incorporate in steps positions with high probability. Reactivity of surface steps could determine the resulting nanostructures. Preferential incorporation in B-type has been already reported[27] and leads to the formation of InAs QDs aligned along [110] direction. We consider that this is the main factor leading to the multiple QD nucleation observed in samples grown at high As_4 flux (F_{eq}(As)=2ML/s or 3.5ML/s) for T_S=490ºC and 510ºC. InAs nucleation at low As_4 flux (F_{eq}(As)=0.5ML/s) differs from higher As_4 fluxes, showing single InAs QD formation, located at the bottom of the nanohole. This suggests that the balance between geometry and reactivity of the steps within the nanohole has changed. The rate of In adatoms net flux on B-type (As terminated) and A-type (Ga terminated) facets within the nanohole is expected to change with As_4 flux[32]. We think that this dependence of In atoms incorporation on As_4 pressure could be related with the observed changes on InAs nucleation. Nevertheless, a more detailed study is necessary for a full understanding of this result.

Occupation statistics for the samples grown under different As_4 conditions is presented in figure 4. Figure 4a shows the probability (%) of obtaining different QD count per pattern site (n=0,1,2,3,4,5) for the three different As_4 overpressures over the large set of fabricated oxide motifs for this work, which includes motifs with oxide radius (r_{ox}) in the range r_{ox}=50-120nm. Figure 4b shows the QD count statistics in a bar plot of three subsets of pattern motifs (r_{ox}=70-80nm, r_{ox}=80-90nm and r_{ox}=90-100nm) for the three different As_4 overpressures under study.

Results plotted on Figure 4 show , on one hand, a clear trend towards single QD occupancy (n=1) when As_4 overpressure decreases and, on the other hand, that high n values become more likely for high As_4 flux. Moreover, for the lower As_4 pressure studied ($F_{eq}(As)$ = 0.5ML/s) single QD occupancy is obtained for the whole range of pattern motif sizes considered on figure 4b. These results demonstrate that the control of the growth kinetics by adjusting the growth parameters during InAs deposition on a patterned substrate leads to the control of the occupation statistics of the InAs QDs formed at the pattern sites.

Zallo et al. have reported on the effect of As rate on the occupancy for nanoholes obtained by droplet epitaxy after growing a thin GaAs buffer layer (10nm)[34]. In that case, the As conditions modify the growth of the buffer layer, and, therefore, the nanohole shape, which results in a shift of the occupation statistics towards single occupancy with increasing As_4 flux, the opposite effect that we observe here. However in the samples presented in this work no buffer layer is grown, all pattern nanoholes undergo the same treatment before InAs growth and no modification in the nanohole geometry is expected; thus, the transition to single QD nucleation should be attributed to modifications on the growth kinetics under low As_4 flux. In this sense, although the reported analysis has been performed on 2μm pitch patterns, it is expected that the result will be valid for different pattern pitch periods. When the pattern pitch is modified, the size of the area surrounding the nanoholes that supplies material for InAs QD nucleation also changes, although no changes in the growth kinetics within the pattern motif are expectable. So we would expect single QD nucleation under the reported growth conditions with independence of the pitch of the pattern. Only the required InAs quantity to successfully complete the single QD nucleation within the nanohole could be different and needed to be adjusted, especially for highly packed patterned substrates.

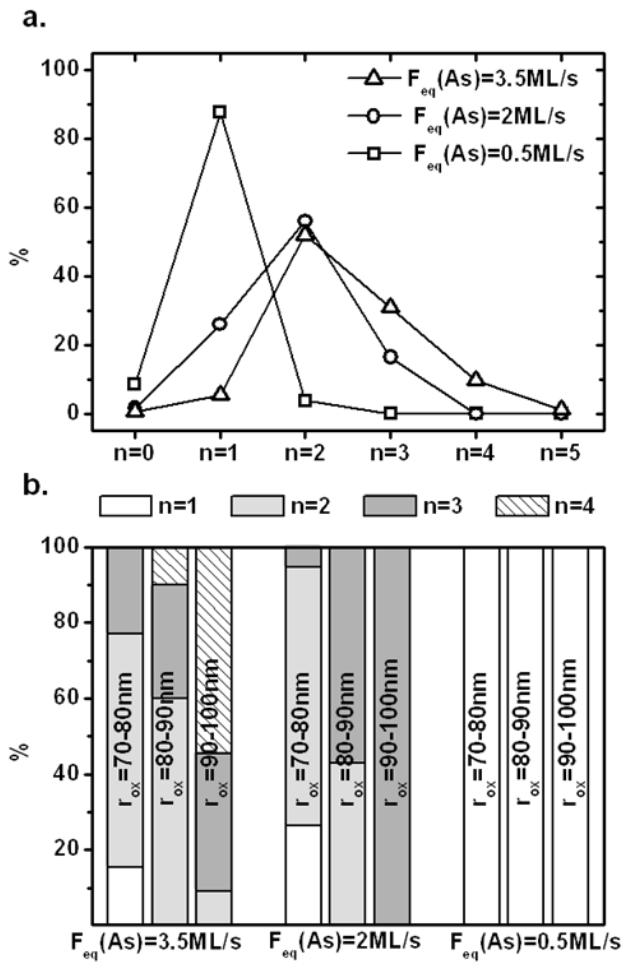

Figure 4. Plot of percentage QD number count per pattern site for the three studied As_4 growth conditions: F_{eq} (As)=0.5ML/s, F_{eq} (As)=2ML/s and F_{eq} (As)=3.5ML/s (a). Occupation bar plot for three subsets sets of oxide motifs: r_{ox}=70-80nm, r_{ox}=80-90nm, and r_{ox}=90-100nm for the three different As_4 overpressures under study (b).

3.3 Vertical stacking of InAs nanostructures

The nanostructures grown right on the patterned surface substrate (re-growth interface), as the ones studied above, are expected to be optically inactive[21,33]. In this sense, it is mandatory to evaluate their capability for being employed as seed nuclei for vertical stacking of optically active nanostructures[14, 33]. With the aim of studying the vertical stacking of InAs nanostructures

and evaluating the optical activity of InAs site-controlled QDs, additional samples were grown. Once the first layer (seed layer) of InAs SCQDs is completed, a GaAs spacer layer is grown and a second InAs layer is deposited, using identical growth parameters as those used at the SCQDs seed layer. These samples were grown at T_S=510ºC under two different As overpressures (F_{eq}(As)=0.5ML/s and F_{eq}(As)=2ML/s) and with a GaAs spacer layer thickness of 15nm and 20 nm. Samples for optical investigation were capped with 125nm thick GaAs layer

AFM morphological characterization of samples with a 15nm thick GaAs spacer layer is presented in figure 5. AFM images of the InAs QD seed layer (figure 5a for F_{eq}(As)=0.5ML/s and 5b for F_{eq}(As)=2ML/s) and the InAs QD stacked layer (figure 5c for F_{eq}(As)=0.5ML/s and 5d for F_{eq}(As)=2ML/s) are shown. Corresponding plots of QD count per pattern site (n=0, 1, 2, 3) for the InAs QD stacked layer are sown in figure 5e and figure 5f. Figure 5e shows that single QD formation per pattern site is achieved with high (~90%) probability for F_{eq}(As)=0.5ML/s, preserving the single QD occupation statistics obtained for such conditions in the seed layer. In contrast, for F_{eq}(As)=2ML/s approximately 50% of pattern sites are occupied by QD pairs. When the GaAs spacer layer thickness is increased to 20nm (not shown), the pattern nucleation selectivity is not successfully propagated up to the potential InAs SCQDs active layer, resulting that QD only nucleate on top of ~20% of pattern sites . This becomes a limitation for the distance between the re-growth interface and the active InAs nanostructures, although it could be overcome by growing larger QD at the seed layer.

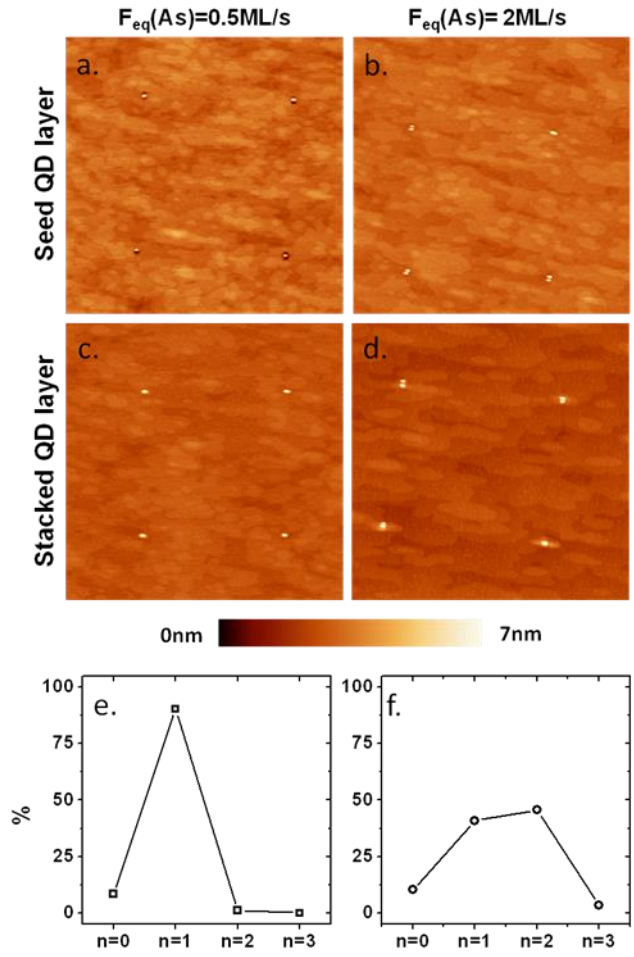

Figure 5. 4x4 μm ^{2} AFM images of InAs QD seed layer (a, b) and InAs QD stacked layer (c, d) grown at T_S=510º and F_{eq}(As)=0.5ML/s or F_{eq}(As)=2ML/s, respectively, with a 15nm thick GaAs spacer layer. Same color scale is used for the four images. Plot of percentage QD number count per pattern site in the InAs QD stacked layer for both As_4 overpressure growth conditions: F_{eq}(As)=0.5ML/s (e) and F_{eq}(As)=2ML/s (f).

Figure 6 present a PL map showing a 5x5 pattern sites region for a sample with 15 nm thick GaAs spacer layer, grown with F_{eq}(As)=0.5ML/s and T_S=510ºC. The map was recorded integrating the PL signal from 900nm up to detector cut-off (~1040nm). An optically active InAs SCQD is found in 88% of the pattern sites, in good agreement with the occupation ratio

evaluated by AFM (figure 5.e), with the emission centered at 1.242 eV. The spectrum of an InAs SCQD (marked with a circle in the PL map) at low excitation power (P_{exc}= 40nW), showing a single spectral line, with full width at half maximum (FWHM) of 81μeV, is shown. This spectral line-width value, in the sub-100 μeV range, is similar to those reported for InAs SCQDs fabricated by other techniques [6, 14], although far from the best reported results where the InAs SCQDs match the optical properties of self assembled InAs QDs [15,16], with spectral line-width values in the sub-10 μeV range. A detailed statistical study of the optical properties of the SCQDs developed in this work will be published elsewhere.

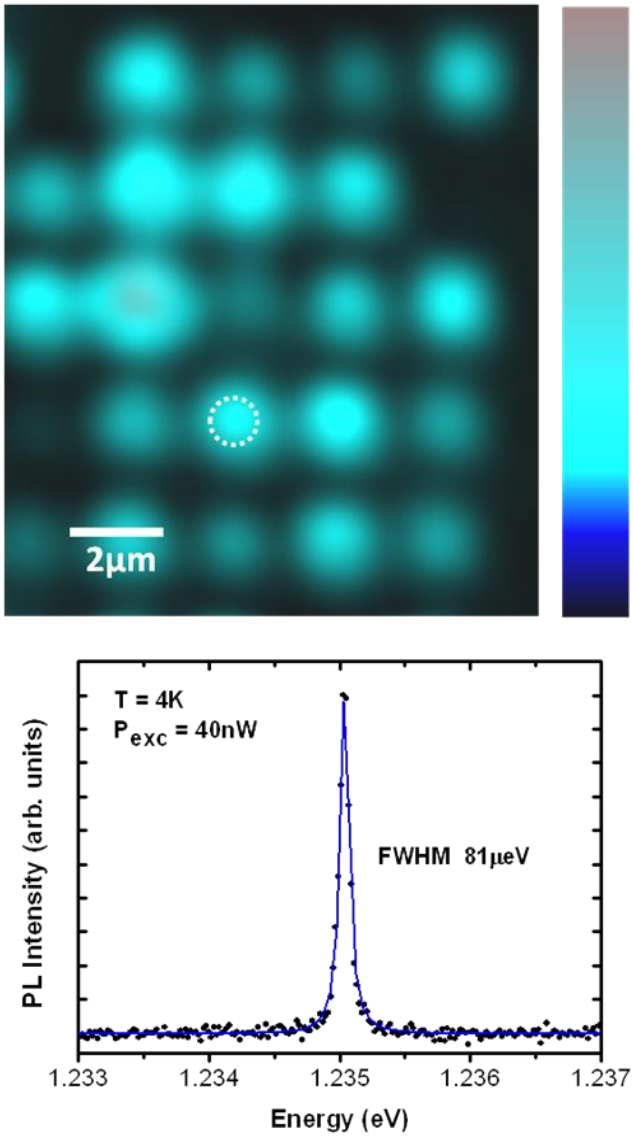

Figure 6. PL map of patterned region showing 5x5 pattern sites and spectrum of single InAs SCQD indicated in the map with the circle. Spectral line-width FWHM is 81µeV.

These results demonstrates that the control of the growth kinetics in the InAs QDs seed layer by adjusting the growth parameters enables the control of the occupation statistics in the stacked InAs QD layer (figure 5). Single QD formation per pattern site, obtained under suitable growth conditions (T_S=510º and F_{eq}(As)=0.5ML/s) in the seed layer, is preserved in the vertically

stacked InAs SCQDs layer for GaAs spacer layer thickness of 15nm. Furthermore, preliminary optical characterization results point out that this procedure produce InAs SCQDs with optical quality comparable to that reported for other fabrication techniques [6, 14]. Undoubtedly there is still room for further optimization of the optical properties of the SCQDs, which could be addressed by means of well-known methods such as the introduction of a AlGaAs blocking layer between the optically active nanostructures and the re-growth interface, or by using reflectors grown below the patterned surface[15]. In this sense, this work presents results of general applicability in the growth of site-controlled InAs QD with good control of the occupation statistics and improved optical emission properties, which is still challenging nowadays.

In general, the reproducible growth of single InAs QDs on GaAs patterned substrates requires a careful control of the pattern site geometry for InAs nucleation. Although control of pattern geometry is crucial, its evolution during the processes previous to InAs deposition is also essential. The buffer layer growth, taking into account growth anisotropy, and annealing process are particularly relevant steps. This has been successfully exploited by Yakes et al. with the growth of positioned InAs QDs with a 90nm thick buffer layer, grown on GaAs substrates patterned by e-beam lithography[16]. Postgrowth annealing is also reported to be a method to modify structural properties of InAs nanostructures grown on patterned substrates and improve single dot occupancy ratio[28]. In the case of InAs QDs grown on GaAs substrates patterned by AFM local oxidation, a fine control of the oxide motif lateral dimensions enables to fabricate single InAs QD or InAs multiple QDs lateral arrangements[27]. In this context, the results presented in this work clearly show that growth parameters (critically As_4 overpressure) are also relevant to control QD number occupation. We have obtained that single dot occupancy can be

achieved in pattern sites without buffer layer with lateral dimensions up to r_{ox}=120nm when the suitable InAs growth parameters are used (T_S=510º and F_{eq}(As)=0.5ML/s). The QD nucleated at the patterned surface can be used as seed layer for an optically active QD grown on top, reproducing the single dot array display. This result provides a robust growth protocol to obtain single site-controlled InAs QDs on patterned substrates.

4. Conclusion

In conclusion, we have studied how the substrate temperature and As_4 overpressure during InAs deposition influence on selective InAs nucleation directly (without GaAs buffer layer growth) on GaAs(001) substrates patterned by AFM local oxidation lithography. Our results show that As_4 overpressure during InAs deposition is a critical parameter in the control of the number of QD formed per pattern site. We demonstrate that multiple InAs QD formation can be avoided in a wide range of pattern site geometry when InAs deposition is carried out at low As_4 overpressure (F_{eq}(As)=0.5ML/s). In this way, the unavoidable evolution of pattern sites into elliptical motifs elongated along [110] during thermal ramp prior to InAs deposition can be ignored and multiple QD nucleation per pattern site avoided. The obtained site control InAs QDs layers can be useful as seed layer for the stacking of optically active site-controlled InAs QDs.

AUTHOR INFORMATION

Corresponding Author

e-mail: jesus@imm.cnm.csic.es

ACKNOWLEDGMENT

The authors thank financial support by Spanish MINECO through grants ENE2012-37804-C02-02 and TEC2011-29120-C05-04. Jesús Herranz acknowledges to the JAE program for the funds.

REFERENCES

(1) Kiravittaya, S.; Rastelli, A.; Schmidt, O. G. *Rep. Prog. Phys.* **2009**, *72*, 046502, and references therein.

(2) O'Brien, J. L.; Furusawa, A.; Vučković, J. *Nat. Photonics* **2009**, *3*, 687–695.

(3) Lan, H.; Ding, Y. *Nano Today* **2012**, *7*, 94–123.

(4) Atkinson, P.; Kiravittaya, S.; Benyoucef, M.; Rastelli, A.; Schmidt, O. G. *Appl. Phys. Lett.* **2008**, *93*, 101908.

(5) Schneider, C.; Heindel, T.; Huggenberger, A.; Weinmann, P.; Kistner, C.; Kamp, M.; Reitzenstein, S.; Höfling, S.; Forchel, A. *Appl. Phys. Lett.* **2009**, *94*, 111111.

(6) Skiba-Szymanska, J.; Jamil, A.; Farrer, I.; Ward, M. B.; Nicoll, C. A.; Ellis, D. J. P.; Griffiths, J. P.; Anderson, D.; Jones, G. A. C.; Ritchie, D. A.; Shields, A. J. *Nanotechnology* **2011**, *22*, 065302.

(7) Tommila, J.; Tukiainen, A.; Viheriälä, J.; Schramm, A.; Hakkarainen, T.; Aho, A.; Stenberg, P.; Dumitrescu, M.; Guina, M. *J. Cryst. Growth* **2011**, *323*, 183–186.

(8) Alonso-González, P.; González, L.; González, Y.; Fuster, D.; Fernández-Martínez, I.; Martín-Sánchez, J.; Abelmann, L. *Nanotechnology* **2007**, *18*, 355302.

(9) Martin, A. J.; Saucer, T. W.; Rodriguez, G. V.; Sih, V.; Millunchick, J. M. *Nanotechnology* **2012**, *23*, 135401.

(10) Song, H. Z.; Usuki, T.; Ohshima, T.; Sakuma, Y.; Kawabe, M.; Okada, Y.; Takemoto, K.; Miyazawa, T.; Hirose, S.; Nakata, Y.; Takatsu, M.; Yokoyama, N. *Nanoscale Res. Lett.* **2006**, *1*, 160–166.

(11) Cha, K. M.; Horiuchi, I.; Shibata, K.; Hirakawa, K. *Appl. Phys. Express* **2012**, *5*, 085501.

(12) Martín-Sánchez, J.; Muñoz-Matutano, G.; Herranz, J.; Canet-Ferrer, J.; Alén, B.; González, Y.; Alonso-González, P.; Fuster, D.; González, L.; Martínez-Pastor, J.; Briones, F. *ACS Nano* **2009**, *3*, 1513–1517.

(13) Albert, F.; Stobbe, S.; Schneider, C.; Heindel, T.; Reitzenstein, S.; Höfling, S.; Lodahl, P.; Worschech, L.; Forchel, A. *Appl. Phys. Lett.* **2010**, *96*, 151102

(14) Huggenberger, A.; Heckelmann, S.; Schneider, C.; Höfling, S.; Reitzenstein, S.;Worschech, L.; Kamp, M.; Forchel, A. *Appl. Phys. Lett.* **2011**, *98*, 131104.

(15) Jöns, K. D.; Atkinson, P.; Müller, M.; Heldmaier, M.; Ulrich, S. M.; Schmidt, O. G.; Michler, P. *Nano Lett.* **2013**, *13*, 126–130.

(16) Yakes, M. K.; Yang, L.; Bracker, A. S.; Sweeney, T. M.; Brereton, P. G.; Kim, M.; Kim, C. S.; Vora, P. M.; Park, D.; Carter, S. G.; Gammon, D. *Nano Lett.* **2013**, *13*, 4870–4875.

(17) Prieto, I.; Herranz, J.; Gonzalez, Y.; Canet-Ferrer, J.; Wewior, L.; Postigo, P. .; Alen, B.; Gonzalez, L.; Kaldirim, M.; Munioz-Camuniez, L.; Fuster, D.; Taboada, A. G.; Ripalda, J. M.; Briones, F.; Munoz-Matutano, G.; Martinez-Pastor, J. In *2011 13th International Conference on Transparent Optical Networks (ICTON)*; **2011**; pp. 1–5.

(18) Prieto, I.; Herranz, J.; Wewior, L.; González, Y.; Alén, B.; González, L.; Postigo, P. A. *Opt. Express* **2013**, *21*, 31615–31622.

(19) Sugaya, T.; Kawabe, M. *Jpn. J. Appl. Phys.* **1991**, *30*, L402–L404.

(20) Bell, G. R.; Kaijaks, N. S.; Dixon, R. J.; McConville, C. F. *Surf. Sci.* **1998**, *401*, 125–137.

(21) Martín-Sánchez, J.; González, Y.; Alonso-González, P.; González, L. *J. Cryst. Growth* **2008**, *310*, 4676–4680.

(22) Sato, K.; Fahy, M. R.; Ashwin, M. J.; Joyce, B. A. *J. Cryst. Growth* **1996**, *165*, 345–350.

(23) Garcia, J. C.; Neri, C.; Massies, J. *J. Cryst. Growth* **1989**, *98*, 511–518.

(24) Ohtake, A.; Ozeki, M. *Appl. Phys. Lett.* **2001**, *78*, 431–433.

(25) Patella, F.; Arciprete, F.; Fanfoni, M.; Balzarotti, A.; Placidi, E. *Appl. Phys. Lett.* **2006**, *88*, 161903.

(26) Heyn, C.; Hansen, W. *J. Cryst. Growth* **2003**, *251*, 218–222.

(27) Martín-Sánchez, J.; Alonso-González, P.; Herranz, J.; González, Y.; González, L. *Nanotechnology* **2009**, *20*, 125302.

(28) Helfrich, M.; Terhalle, B.; Ekinci, Y.; Schaadt, D. M. *J. Cryst. Growth* **2013**, *371*, 39–44.

(29) Kiravittaya, S.; Heidemeyer, H.; Schmidt, O. G. *Phys. E Low-Dimens. Syst. Nanostructures* **2004**, *23*, 253–259.

(30) Heyn, C.; Endler, D.; Zhang, K.; Hansen, W. *J. Cryst. Growth* **2000**, *210*, 421–428.

(31) Yang, B.; Liu, F.; Lagally, M. G. *Phys. Rev. Lett.* **2004**, *92*, 025502.

(32) Shen, X. Q.; Nishinaga, T. *J. Cryst. Growth* **1995**, *146*, 374–378.

(33) Huggenberger, A.; Schneider, C.; Drescher, C.; Heckelmann, S.; Heindel, T.; Reitzenstein, S.; Kamp, M.; Höfling, S.; Worschech, L.; Forchel, A. *J. Cryst. Growth* **2011**, *323*, 194–197.

(34) Zallo, E.; Atkinson, P.; Rastelli, A.; Schmidt, O. G. *J. Cryst. Growth* **2012**, *338*, 232–238.

For Table of Contents Use Only

Study of growth parameters for single InAs QD formation on GaAs (001) patterned substrates by local oxidation lithography.

Jesús Herranz, Luisa González and Yolanda González

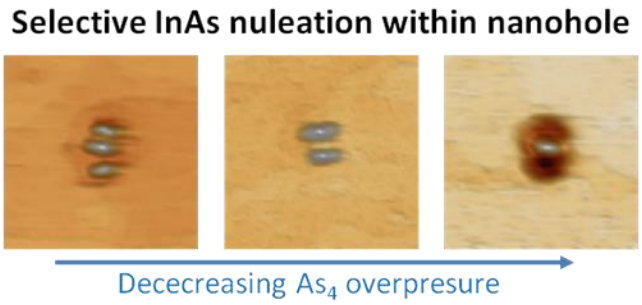

This work studies the selective nucleation of InAs within nanoholes on GaAs(001) substrates patterned by atomic force microscopy local oxidation. Effects of substrate temperature and As_4 overpressure are considered. When InAs is deposited under low As_4 overpressure at substrate temperature of T_S=510ºC, single InAs quantum dot per nanohole is obtained for a broad range of sizes of pattern motifs.